Throughput Maximization in MIMO Cognitive Radio Networks with SWIPT DF Relay and Imperfect CSI

Mahla Mohammadi, Seyed Mehdi Hosseini Andargoli*

Department of Electrical and Computer Engineering, Babol Noshirvani University of Technology, Babol, Iran.
mahla.mohammadi@stu.nit.ac.ir, smh_andargoli@nit.ac.ir*
*Corresponding author

Received: 06/03/2023, Revised:16/05/2023, Accepted: 14/10/2023.

Abstract
We address the throughput maximization problem for downlink transmission in DF-relay-assisted cognitive radio networks (CRNs) based on simultaneous wireless information and power transfer (SWIPT) capability. In this envisioned network, multiple-input multiple-output (MIMO) relay and secondary user (SU) equipment are designed to handle both radio frequency (RF) signal energy harvesting and SWIPT functional tasks. Additionally, the cognitive base station (CBS) communicates with the SU only via the MIMO relay. Here, several combined constraints of the main problem complicate the solution. Therefore, we apply heuristic guidelines within the convex optimization framework to handle this complexity. First, consider the problem of maximizing throughput on both sides of the relay separately. Second, each side progresses to solve the complex problem optimally by adopting strategies for solving sub-problems. Finally, these optimal solutions are synthesized by proposing a heuristic iterative power allocation algorithm that satisfies the combinatorial constraints with short convergence times. The performance of the optimal proposed algorithm (OPA) is evaluated against benchmark algorithms via numerical results. The OPA is about 10000 times faster than the CVX solver. Additionally, the sum throughput especially at low thresholds increases by ~15-25% compared to the benchmark algorithms. Moreover, the constraints and objective function in OPA are 100% satisfied.

Keywords
Throughput maximization, cognitive radio, DF relay, SWIPT, MIMO.

1. Introduction

As the number of wireless devices grows rapidly, the demand for frequency spectrum usage increases in each era of communication, so concerns about spectrum scarcity remain a key issue in 5G and 6G technologies [1]. To solve this problem, cognitive radio (CR) has been proposed as a preferred technology for the efficient use of the spectrum [2, 3]. In contrast to assigning frequencies to licensed users as primary users (PUs) on a fixed basis, the CR allows unlicensed users as secondary users (SUs) to access the spectrum of PUs through spectrum sharing paradigms [4]. Therefore, the transmitter of SU as a cognitive base station (CBS) should prevent harmful interference to PU [5]. The networks based on CR technology continuously monitor the spectrum to determine when spectrum band is suitable for SU. Hence, this process increases power consumption. On the other hand, charging or replacing standard batteries is very expensive and inefficient. Providing sufficient energy in such energy-constrained systems is a major challenge [6].

Recently, the concept of radio frequency (RF) energy harvesting has been introduced as a stable and reliable power source to extend the life of wireless devices with little or no power supply. In particular, simultaneous wireless information and power transfer (SWIPT) technology for energy harvesting (EH) is of great interest in 5G communications [7]. Based on SWIPT technique, there are two practical receiver schemes called power splitting (PS) and time switching (TS). In the PS scheme, the received signal is split into two different power streams with adjustable power ratios. One of power streams is for EH and another one is for information decoding (ID). In the TS scheme, the receiver alternates between decoding information and harvesting energy at each time slot. In general, PS protocol achieves a better rate-energy transmission trade-off and lower transmission delay than TS protocol [8]. This encouraged the use of SWIPT in cognitive radio networks (CRNs) [9, 10].

Additionally, with the evolving requisition for higher throughput transmissions, especially in CRNs, the multiple-input multiple-output (MIMO) structure can provide a suitable solution by exploiting spatial multiplexing gain [11]. The increased spatial degree of freedom (DoF) of MIMO structures also improve the energy efficiency of EH-based networks [12]. On the other side, one of the key challenges in signal transmission between source and destination is the unreliability of direct connections due to obstructions or other reasons. To overcome this problem, relays can be

used as intermediate devices with SWIPT technique for signal transmission [13, 14].

As one of the main concerns of emerging technologies in the next few years is to ensure secure communication with low power consumption, complexity, cost, and high throughput transmission. For these reasons, the present research examined MIMO CRNs with SWIPT decode-and-forward (DF) relay and imperfect channel state information (CSI) to provide an efficient power allocation algorithm.

1.1. Prior works

Considering the characteristics and advantages of MIMO SWIPT-capable relay-based CRNs, it became an incentive to examine these networks in different aspects, such as maximizing the sum throughput, resource allocation, and so on.

EH-capable CR-free relay systems are discussed in some studies [14, 15-20]. The authors in [15] studied the MIMO SWIPT relaying system with a direct link. They proposed an optimal PS matrix design to maximize the achievable sum-rate of the system where the PS factors of different relay's antennas are different. In [16], the single antenna multi-user relay-assisted scenario has been considered based on the orthogonal frequency division multiple access (OFDMA) communication. Accordingly, the suboptimal algorithm has been presented for relay selection and power allocation based on the amplify-and-forward (AF) relays and PS-capable destinations with perfect CSI. To maximize the overall sum rate of the system, they also considered the limitations on the transmit power and harvested energy.

The authors in [14] investigated a new energy consumption manner as a harvest-store-consume (HSC) model for transmission via direct and wireless-powered relay links within multiple frames' periods. Then, the time allocation algorithm has been proposed to attain the best average throughput in a single antenna EH-capable relay system. In [17], the throughput maximization problem has been formulated for SWIPT-capable full-duplex relay subject to power restrictions in MIMO communication system. Based on the Lagrange duality theory, they proposed an algorithm for non-uniform PS factor assignment and optimal power allocation through the subgradient method.

Based on a dual-hop DF MIMO EH-relay system, the source-destination mutual information (MI) maximization problem has been formulated in [18]. There, the energy constraints have been considered to optimize the TS factor, PS factor, and source and relay covariance matrices. Owing to the complexity of the main problems, they proposed two algorithms based on decomposing the original problems into simpler convex subproblems. These algorithms solved the problems through the primal-dual interior-point method. The authors in [19] considered a multi-user MIMO DF relay system where the relays are based on SWIPT-capable TS protocol. As the MIMO channel capacity maximization requires a high level of computational complexity, they used the block diagonalization (BD) method at the source and reframed the sum-rate maximization problem as a convex optimization problem. Then, CVX software was used to optimize the power allocation at relays and destinations. The relays are battery-free nodes with perfect CSI.

The MIMO DF relaying system has been considered based on SWIPT-capable PS protocol in [20]. The authors formulated the achievable throughput maximization problem in three scenarios to optimize the power allocation and PS factor assignment in all links at the relay(s). Accordingly, the novel algorithms were proposed for power and PS factor assignment based on convex optimization algorithms. The authors in [21] proposed a low-complexity closed-form formula for the outage probability of the energy-harvested direct and DF relay-aided underlay device-to-device communications in Nakagami fading channel. The proposed closed-form expression is valid for both energy-harvested and non-energy-harvested scenarios. Also, the formula is based on n-point generalized Gauss-Laguerre and m-point Gauss-Legendre solutions.

Cognitive radio networks have been explored with some capabilities in several research studies for different purposes [22-28]. The work [22] has been investigated the performance of the multi-user underlay EH-CRN. The minimization of asymptotic outage probability problem is formulated under the network constraints. Then, the closed-form expressions provided for the exact outage probability of the network, the average symbol error probability, and ergodic capacity.

Based on the harvest-then-transmit protocol, the sum throughput maximization problems have been formulated in the context of the underlay and overlay single antenna CRN in [23] with perfect CSI. The authors provided two sum throughput maximization algorithms with separate optimization on time and power by dividing the main problems into two subproblems. Furthermore, the authors in [24] extend the work of [23] to the MIMO-based CRN. There, an ellipsoid algorithm recruited to optimize the beamforming (BF) covariance matrices. In these works, there is a time lag in energy harvesting and no synchronicity between information transmission and energy harvesting.

The authors in [25] tried to propose new beamforming and power allocation strategy in a multiple-input single-output (MISO) CR downlink network based on PS protocol with perfect CSI. Finally, they used CVX software to solve a simplistic optimization problem to maximize the minimum achievable rate among users. The MIMO-OFDMA-based CRN was well investigated in our previous studies [26-28]. To maximize the sum throughput in two spectrum sharing overlay and underlay models, we introduced the heuristic optimal and suboptimal algorithms for power and subcarrier assignment. The algorithms are also desirable in terms of efficiency. Moreover, there are some study with different objective functions, optimization variables, and different networks such as minimization of the total transmit power of users in uplink multi-unmanned aerial vehicle (UAV) wireless communication network [29], a queue management policy to enhance the quality of service of CRN [30]. These works are not based on SWIPT-relay CRN and MIMO SWIPT-relay structure, respectively. In addition, the analysis of outage and average symbol error probability in MIMO SWIPT relay

network with imperfect CSI [31] but not in CRN with sum throughput maximization. The authors in [32] optimized the sum-rate constrained by consumed power for multi antenna non-regenerative relay network. This paper is not based on SWIPT CRN.

1.2. Novelty and contributions

The technologies such as CR and SWIPT were highly considered in the present and next generation of telecommunication. On the other hand, the CR-based networks have interference constraints, which complicate problem solving. Therefore, using the PUs' spectrum and pay attention to new technologies at the same time is an important issue that must be addressed [1]. Moreover, in high density closed environments with obstacles that there is no direct link between the transmitter and receiver, the idea of using relay (as interface device for data transmission) is an another key technology in the next generation of telecommunication [17][19]. Additionally, SWIPT based on the PS scheme ensures simultaneous data transmission and energy harvesting, so separate time is not spent for these operations and part of the throughput does not decrease. This topic is a practical scenario because in present and next generations of the telecommunication, we have to use the available spectrum due to the many requests for high data throughput. On the other hand, it is desirable that the maximum throughput of the network can be achieved.

With the background of the aforementioned prior works, there is still no study that focuses on the throughput maximization of MIMO SWIPT-enabled relay-based CRNs. In this paper, the downlink sum throughput of the MIMO SWIPT-enabled relay-assisted CR network is maximized while the induced interference on PU, the total transmitted powers from CBS and relay, and the harvested energy in relay guarantee their own pre-set threshold. Accordingly, we formulate the resource allocation problem based on the network restrictions. There are two critical challenges in this problem that arise from the combinatorial constraints and make it difficult to solve. One is that the interference induced by both cognitive base station (CBS) and relay on the primary network should be jointly below the interference threshold. Another one is that the powers allocated to the relay-SU link depend on the powers assigned to subchannels of the CBS-relay links. By these drawbacks, we propose an innovative procedure based on the convex optimization framework that confirms the fulfilment of the constraint sets. For further explanation, by dividing the original problem into two convex problems for the two sides of the relay device, we obtain the allocated power in each side by using the subproblems-solving strategy based on Karush-Kuhn-Tucker (KKT) conditions and the subgradient-based searches. Here, the idea of our work becomes clearer that somehow these solutions are used in the main body of the proposed algorithm while ensuring all constraints. Moreover, comparing the proposed algorithm with the benchmark algorithms confirms its good efficiency in terms of optimality, compliance with constraints, and convergence time.

The remaining sections of this article are structured as follows. Section 2 describes the MIMO SWIPT relay-assisted cognitive radio network structure and the problem formulation. Detailed concepts and the solution framework are outline in section 3 and section 4 evaluates the efficiency of the proposed algorithm via numerical simulations. Eventually, section 5 concludes the article.

2. Network structure and problem formulation

As depicted in Fig. 1, we consider a MIMO DF relay-assisted SWIPT CR network. A primary network and a secondary network operate simultaneously based on the underlay spectrum sharing model. In the primary network, there are a primary base station (PBS) and a PU with a single antenna. The secondary network consists of a CBS with N_T antennas, a relay with N_R antennas, and a single-antenna SU. Additionally, the relay and SU harvest RF energy based on the PS protocol, whereas the relay is a battery-free device. Owing to the severe path attenuation or shadowing effect of obstacles, the CBS can communicate with SU just through the relay.

Similar to [23] and [24], the global channel state information (CSI) of the secondary and primary networks are available in CBS. Under this assumption, the singular value decomposition (SVD) technique can be recruited in the point-to-point MIMO link between CBS and relay to provide the maximum throughput [33]. For better clarity, the descriptions of all formulas' symbols are given in Table I.

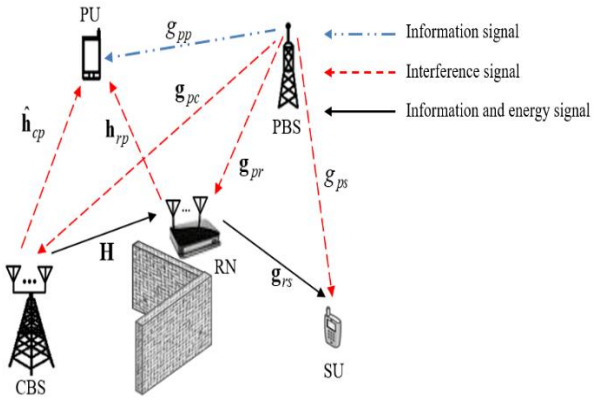

Fig. 1. The MIMO DF relay-assisted SWIPT CR network model

Hence, the MIMO channel matrix for dense scattering Rayleigh CBS-relay links $\mathbf{H} \in \mathrm{C}^{N_R \times N_T}$ can be decomposed as

$$\mathbf{H} = \mathbf{U}\ \mathbf{\Lambda}^{1/2}\ \mathbf{V}^H, \tag{1}$$

where $\mathbf{V} \in \mathrm{C}^{N_T \times L}$ and $\mathbf{U} \in \mathrm{C}^{N_R \times L}$. $\mathbf{\Lambda} \in \mathrm{R}_+^{L \times L}$ is diagonal singular values matrix $L = \min(N_T, N_R)$. The precoding matrix $\mathbf{V}$ multiplies by power-allocated information signal vector of CBS, whereas the received signal in ID receiver of the relay multiplies by $\mathbf{U}^H$.

Table I. Descriptions of all formulas' symbols

Symbol	Description	Symbol	Description
$\mathcal{CN}(\mu,\sigma^2)$	Circularly symmetric complex normal distribution with mean μ and variance σ^2	$\mathrm{R}_+^{n\times n}$	The $n\times n$ matrix with positive real elements
$\mathbf{I}_n$	The $n\times n$ identity matrix	$\mathrm{C}^{n\times n}$	The $n\times n$ matrix with complex elements
diag(.)	Diagonal matrix	C	Complex number
E{.}	Statistical expectation operator	T	frame time
$\mathbf{H}$	The MIMO channel matrix for CBS-relay links	L	The number of parallel independent subchannels
$\mathbf{V}$	Unitary matrix for precoding BF at CBS	N_T	The number of CBS antennas
$\mathbf{U}$	Unitary matrix for postcoding BF at relay	N_R	The number of relay antennas
$\mathbf{\Lambda}$	Diagonal singular values matrix	p_r	The power allocated to the SU
$\mathbf{x}$	The transmitted normalized baseband information data symbols from CBS to relay	p_l	The power allocated to the *l*th parallel independent subchannel
s_p	The transmitted normalized baseband information data symbol from PBS to PU	P_T	The total power budget of CBS
$\mathbf{n}$	The effective noise vector at the relay	P_p	The transmit power of PBS
$\mathbf{n}_{id}$	ID analog circuit's internal noise vector	I_{pu}	The tolerable interference power of PU
$\mathbf{n}_{rf}$	The received noise vector at relay's antennas	ζ	The energy harvesting efficiency at the relay
$\mathbf{g}_{pr}$	The baseband channel vector of PBS-relay link	ρ	The power splitting factor at the relay's antenna
$\mathbf{g}_{rs}$	The baseband channel vector of relay-SU link	θ	The power splitting factor at the SU's antenna
g_{ps}	The baseband channel of PBS-SU link	σ^2	The effective noise power at each antennas of the relay
$\hat{\mathbf{h}}_{cp}$	The channel vector of CBS-PU link	σ_s^2	The effective noise power at the SU
$\mathbf{h}_{rp}$	The channel vector of relay-PU link	$\sigma_{rf}^2, \sigma_{rf,s}^2$	The power of received noise at relay and SU
$\mathbf{h}_{cp}$	The effective interference channel vector of CBS-PU link	$\sigma_{id}^2, \sigma_{id,s}^2$	The power of internal noise at relay and SU
$h_{cp,l}$	The effective interference channel coefficient between *l*th spatial subchannel of CBS and PU		

Hence, the two baseband signals $\mathbf{y}_{EH} \in \mathrm{C}^{N_R\times 1}$ in the EH receiver and $\mathbf{y}_{ID} \in \mathrm{C}^{N_R\times 1}$ in the ID receiver can be written as

$$\mathbf{y}_{EH} = \mathbf{\Sigma}_\rho^{1/2}\mathbf{H}\,\mathbf{V}\,\mathbf{P}^{1/2}\mathbf{x} + \mathbf{\Sigma}_\rho^{1/2}P_p^{1/2}\,\mathbf{g}_{pr}\,s_p\,, \tag{2}$$

$$\mathbf{y}_{ID} = (\mathbf{I}-\mathbf{\Sigma}_\rho)^{1/2}\mathbf{H}\,\mathbf{V}\,\mathbf{P}^{1/2}\mathbf{x} + (\mathbf{I}-\mathbf{\Sigma}_\rho)^{1/2}P_p^{1/2}\,\mathbf{g}_{pr}\,s_p + (\mathbf{I}-\mathbf{\Sigma}_\rho)^{1/2}\mathbf{n}_{rf} + \mathbf{n}_{id}\,, \tag{3}$$

where $\mathbf{x}\sim\mathcal{CN}(0,\mathbf{I}_L)$, $s_p\sim\mathcal{CN}(0,1)$, $\mathbf{g}_{pr}\in\mathrm{C}^{N_R\times 1}$, $\mathbf{n}_{rf}\sim\mathcal{CN}(0,\sigma_{rf}^2\mathbf{I}_{N_R})$ and $\mathbf{n}_{id}\sim\mathcal{CN}(0,\sigma_{id}^2\mathbf{I}_{N_R})$. Also, $\mathbf{P}=\mathrm{diag}(p_1,p_2,\ldots,p_L)\in\mathrm{R}_+^{L\times L}$ and $\Sigma_\rho=\mathrm{diag}(\rho_1,\rho_2,\ldots,\rho_{N_R})\in\mathrm{R}_+^{N_R\times N_R}$ are diagonal matrices in which $\rho_i\in(0,1)$. Based on the equal PS factor assumption in (2) and (3), the average harvested energy over $T=1\,\mathrm{s}$ and the postcoded ID receiver signal can be rewritten as

$$P_{EH}(\mathbf{P}) = \zeta\rho\mathrm{E}\{\mathbf{x}^H\mathbf{P}^{1/2}\overbrace{\mathbf{V}^H\mathbf{H}^H\mathbf{H}\,\mathbf{V}}^{\mathbf{\Lambda}}\mathbf{P}^{1/2}\mathbf{x}\} + \zeta\rho P_p\,\|\,\mathbf{g}_{pr}\,\|^2 = \zeta\rho\left((\sum_{l=1}^{L}\Lambda_l\,p_l) + P_p\,\|\,\mathbf{g}_{pr}\,\|^2\right), \tag{4}$$

$$\mathbf{y} = \mathbf{U}^H\mathbf{y}_{ID} = (1-\rho)^{1/2}\mathbf{\Lambda}^{1/2}\,\mathbf{P}^{1/2}\,\mathbf{x} + (1-\rho)^{1/2}\mathbf{U}^H(P_p^{1/2}\,\mathbf{g}_{pr}\,s_p) + \mathbf{U}^H\mathbf{n}\,, \tag{5}$$

where $0<\zeta\le 1$ and $\mathbf{n}\sim\mathcal{CN}(0,((1-\rho)\sigma_{rf}^2+\sigma_{id}^2)\mathbf{I}_{N_R})$. Let us denote $\sigma^2=(1-\rho)\sigma_{rf}^2+\sigma_{id}^2$. Similar to our prior studies [27] and [28], $\mathbf{h}_{cp}\in\mathrm{C}^{1\times L}$ can be modeled as

$$\mathbf{h}_{cp} = \hat{\mathbf{h}}_{cp}\mathbf{V}\,, \tag{6}$$

where $\hat{\mathbf{h}}_{cp} \in \mathrm{C}^{1\times N_T}$. The PU receives interferer CBS signals with the total power $\mathrm{E}\{|\hat{\mathbf{h}}_{cp}\mathbf{V}\,\mathbf{P}^{1/2}\mathbf{x}|^2\} = \sum_{l=1}^{L}|h_{cp,l}|^2\ p_l$. It is noteworthy that the simulation is also done assuming imperfect CSI on $\hat{\mathbf{h}}_{cp}$. Based on the underlay spectrum sharing model, the power allocation at CBS must be designed to satisfy the constraint $\sum_{l=1}^{L}|h_{cp,l}|^2\ p_l \le I_{pu}$. From the CBS power budget issue, the power allocation is constrained to $\sum_{l=1}^{L} p_l \le P_T$. Based on (5), the sum throughput of the CBS-relay link is obtained as [33]

$$R_{cr} = \sum_{l=1}^{L}\log_2\left(1+\frac{(1-\rho)\Lambda_l\ p_l}{\sigma^2+(1-\rho)P_p\left\|\mathbf{g}_{pr}\right\|^2}\right). \quad (7)$$

Besides, the optimum linear precoding $\frac{\mathbf{g}_{rs}}{\left\|\mathbf{g}_{rs}\right\|}$ can be used at the relay to maximize the throughput of the MISO channel between relay-SU links [34]. Therefore, the sum throughput of the relay-SU link can be written as

$$R_{rs} = \log_2\left(1+\frac{(1-\theta)\ p_r\left\|\mathbf{g}_{rs}\right\|^2}{\sigma_s^2+(1-\theta)P_p\ |g_{ps}|^2}\right), \quad (8)$$

where $\mathbf{g}_{rs} \in \mathrm{C}^{1\times N_R}$, $\mathrm{g}_{ps} \in \mathrm{C}$, and $\theta \in (0,1)$. Let us denote $\sigma_s^2 = (1-\theta)\sigma_{rf,s}^2 + \sigma_{id,s}^2$.

Similar to CBS, the relay is also restricted to limit its produced interference. The interference generated by the relay on the PU can be written as $p_r\,\|\mathbf{h}_{rp}\|^2$ in which $\mathbf{h}_{rp} \in \mathrm{C}^{1\times N_R}$. So, the power allocation at the relay is subjected to $p_r\,\|\mathbf{h}_{rp}\|^2 \le I_{pu}$. From the relay power budget perspective, the assigned power is limited to average harvested power as $p_r \le P_{EH}(\mathbf{P})$.

Due to the DF relay, the network throughput can be calculated based on the minimum of (7) and (8) [35]. Without loss of generality, the objective function can be formulated as $\max\{\min(R_{cr},R_{rs})\} = \max\{R\}$. Thus, the optimization problem can be written as

$$(\mathrm{P1}) \max_{\{p_l\},p_r,R} \quad R$$

$$\text{s.t. } \sum_{l=1}^{L} p_l \le P_T, \quad (9)$$

$$\sum_{l=1}^{L}|h_{cp,l}|^2\ p_l \le I_{pu}, \quad (10)$$

$$p_r \le \zeta\rho\left((\sum_{l=1}^{L}\Lambda_l\ p_l)+P_p\,\|\mathbf{g}_{pr}\|^2\right), \quad (11)$$

$$p_r\,\|\mathbf{h}_{rp}\|^2 \le I_{pu}, \quad (12)$$

$$R \le R_{cr}, \quad (13)$$

$$R \le R_{rs}, \quad (14)$$

$$p_l \ge 0,\ \forall\ l \in \{1,2,...,L\}, \quad (15)$$

$$p_r \ge 0. \quad (16)$$

Since the functions (7) and (8) are concave on $\{p_l\}$ and p_r, the constraints (13) and (14) will be convex sets. Also, the other constraints are affine functions. Hence, we can easily conclude that (P1) is a convex problem on optimization variables. Due to the simultaneous satisfaction of all constraints and the existence of the coupled optimization variables in constraint (11), it may be difficult to solve the problem (P1) optimally with reasonable complexity in standard form. Nevertheless, we propose a novel solution to handle the complexities that can efficiently compute an optimum solution with a low convergence time.

3. Optimal solution framework

To make the problem (P1) more tractable, we first divide (P1) into two separate problems so that the optimum solution of the first problem is considered as a constraint in the second one. Hence, the first problem is formulated to maximize the sum throughput of the CBS-relay link by optimizing the downlink power allocation in section 3.1. As a second problem, the sum throughput of the relay-SU link is maximized in section 3.2. Then, in section 3.3, we will determine the optimal statements based on the derived solutions to frame the proposed algorithm.

3.1. Maximizing throughput of the CBS to relay link

The first throughput maximization problem in CBS-relay link can be formulated as

$$(\mathrm{P2}) \max_{\{p_l\}} R_{cr} \quad \text{s.t. } (9),(10),(15). \quad (17)$$

With convexity, we can solve the problem based on the Lagrangian duality method [36]. The Lagrangian of (P2) is expressed as

$$L(\{p_l\},\psi,\xi,\{\mu_l\}) = -\sum_{l=1}^{L}\log_2\left(1+\frac{(1-\rho)\Lambda_l\ p_l}{\sigma^2+(1-\rho)P_p\left\|\mathbf{g}_{pr}\right\|^2}\right)$$
$$+\psi\left(\sum_{l=1}^{L}p_l - P_T\right)+\xi\left(\sum_{l=1}^{L}|h_{cp,l}|^2\ p_l - I_{pu}\right)-\sum_{l=1}^{L}\mu_l p_l, \quad (18)$$

where ψ, ξ, and $\{\mu_l\}$ denote the non-negative Lagrangian dual variables cognate with the constraints (9), (10), and (15), respectively. Given the combinatorial constraints (9) and (10), our proposed strategy in [27] can be employed here to find the optimal power allocation. Therefore, the problem (P2) is divided into two subproblems as the constrained power budget problem

$$\max_{\{p_l^{sub1}\}} R_{cr,sub1} \quad \text{s.t. } (9),(15), \quad (19)$$

and the constrained interference power problem,

$$\max_{\{p_l^{sub2}\}} R_{cr,sub2} \quad \text{s.t. } (10),(15), \quad (20)$$

where $R_{cr,sub1}$ and $R_{cr,sub2}$ are computed by substituting $\{p_l^{sub1}\}$ and $\{p_l^{sub2}\}$ instead of $\{p_l\}$ in (7), respectively. Since (19) and (20) are also convex problems, the optimum solutions are obtained based on the Lagrangian method and the KKT optimality conditions as follows

$$p_l^{sub1*} = \left(\frac{1}{ln\,2(\eta)} - \frac{\sigma^2 + (1-\rho)P_p \left\| \mathbf{g}_{pr} \right\|^2}{(1-\rho)\Lambda_l} \right)^+, \quad (21)$$

$$p_l^{sub2*} = \left(\frac{1}{ln\,2(\gamma\,|h_{cp,l}|^2)} - \frac{\sigma^2 + (1-\rho)P_p \left\| \mathbf{g}_{pr} \right\|^2}{(1-\rho)\Lambda_l} \right)^+, \quad (22)$$

where the non-negative Lagrangian dual variables η and γ are set to satisfy the power budget and interference power constraints with equality as $\sum_{l=1}^{L} p_l^{sub1*} = P_T$ and $\sum_{l=1}^{L} |h_{cp,l}|^2\ p_l^{sub2*} = I_{pu}$, respectively. Let us denote $(\mathrm{x})^+ = \max(\mathrm{x}, 0)$. It is noteworthy that the two separate bisection algorithms can be applied for iterative updating η and γ with guaranteed convergence [36]. Based on these solutions, we determine the optimum solution of (P2) as $\{p_l^{a*}\}$ in the following Lemmas.

Lemma 1: If substituting $\{p_l^{sub1*}\}$ in (10) satisfies the inequality as $\sum_{l=1}^{L} |h_{cp,l}|^2\ p_l^{sub1*} \le I_{pu}$, $\{p_l^{a*}\} = \{p_l^{sub1*}\}$ is the global optimum solution. Otherwise, $\{p_l^{sub2*}\}$ replaces in (9) and if the constraint is met as $\sum_{l=1}^{L} p_l^{sub2*} \le P_T$, the global optimum solution is $\{p_l^{a*}\} = \{p_l^{sub2*}\}$. If Lemma 1 is not established, the optimum solution $\{p_l^{a*}\}$ cannot be obtained based on the subproblems' solutions. Hence, the following Lemma 2 should be used here.

Lemma 2: the optimal power allocation $\{p_l^{a*}\}$ must be determined to jointly meet the constraints (9) and (10) in (P2) with equality. From (18), the optimal power allocation $\{p_l^{a*}\}$ can be specified as

$$p_l^{a*} = \left(\frac{1}{ln\,2(\psi + \xi\,|h_{cp,l}|^2)} - \frac{\sigma^2 + (1-\rho)P_p \left\| \mathbf{g}_{pr} \right\|^2}{(1-\rho)\Lambda_l} \right)^+, \quad (23)$$

where the non-negative Lagrangian dual variables ψ and ξ are defined in a way that these two equalities $\sum_{l=1}^{L} p_l^{a*} = P_T$ and $\sum_{l=1}^{L} |h_{cp,l}|^2\ p_l^{a*} = I_{pu}$ are met simultaneously. The iterative ellipsoid search is used to update ψ and ξ with guaranteed convergence to the global optimum point [36]. Based on the Lemma 1 and Lemma 2, R_{cr}^1 can be defined as

$$R_{cr}^1 = \sum_{l=1}^{L} \log_2 \left(1 + \frac{(1-\rho)\Lambda_l\ p_l^{a*}}{\sigma^2 + (1-\rho)P_p \left\| \mathbf{g}_{pr} \right\|^2} \right). \quad (24)$$

3.2. Maximizing throughput of the relay to SU link

Furthermore, the second throughput maximization problem in the relay-SU link can be framed as

$$\text{(P3)} \ \max_{p_r} \ R_{rs} \ \text{s.t. (11), (12), (16).} \quad (25)$$

It is noteworthy that the solution of the (P3) relies on the solution of the (P2) through the constraint (11). Hence, power allocation p_r^{b*} is determined after assigning $\{p_l^{a*}\}$. Based on KKT conditions, we can easily find p_r^{b*} and R_{rs}^2 as

$$p_r^{b*} = min\left(\zeta\rho \left(\left(\sum_{l=1}^{L} \Lambda_l\ p_l^{a*} \right) + P_p \left\| \mathbf{g}_{pr} \right\|^2 \right), \frac{I_{pu}}{\left\| \mathbf{h}_{rp} \right\|^2} \right). \quad (26)$$

$$R_{rs}^2 = \log_2 \left(1 + \frac{(1-\theta)\ p_r^{b*} \left\| \mathbf{g}_{rs} \right\|^2}{\sigma_s^2 + (1-\theta)P_p\,|g_{ps}|^2} \right). \quad (27)$$

From these two subsections, the optimal power allocations $\{p_l^{a*}\}$ and p_r^{b*} definitely meet the optimal KKT conditions of the (P1) constraints (9)-(12), (15), and (16). Given that the main problem (P1) is solved separately in sections 3.1 and 3.2, there is no assurance that R will be maximized. Accordingly, the optimal KKT conditions for the original problem (P1) must be met as

$$p_l^* = \left(\frac{\alpha}{ln\,2(\psi_1 + \xi_1\,|h_{cp,l}|^2 - \lambda\zeta\rho\Lambda_l)} - \frac{\sigma^2 + (1-\rho)P_p \left\| \mathbf{g}_{pr} \right\|^2}{(1-\rho)\Lambda_l} \right)^+, \quad (28)$$

$$p_r^* = min\left(\zeta\rho \left(\left(\sum_{l=1}^{L} \Lambda_l\ p_l^* \right) + P_p \left\| \mathbf{g}_{pr} \right\|^2 \right), \frac{I_{pu}}{\left\| \mathbf{h}_{rp} \right\|^2} \right), \quad (29)$$

$$\alpha(R - R_{cr}) = 0, \quad (30)$$

$$\beta(R - R_{rs}) = 0, \quad (31)$$

$$\alpha + \beta = 1, \quad (32)$$

where ψ_1, ξ_1, λ, α, and β are the non-negative Lagrangian dual variables cognate with the constraints (10)-(12), (14), and (15), respectively. Based on (30)-(32) and the non-negativity of (28), it can be easily concluded that the optimum solutions are $0 \le \alpha < 1$ and

$$R_{cr} \ge R_{rs} = R. \quad (33)$$

In the following subsection, we checked the channels' condition on both sides of the relay to ensure that (33) could be met satisfactorily. Hence in terms of channels' condition, we propose three feasible propositions based on throughputs R_{cr}^1 and R_{rs}^2. This process ensures convergence to the optimum point along with a significant reduction in time.

3.3 Proposed algorithm with optimal statements

According to R_{cr}^1 and R_{rs}^2, three feasible propositions are expressed as follows.

$$\{p_l^{EH*}\}=\begin{cases} p_y^{EH*}=P_T,\ p_x^{EH*}=0\ \forall x\neq y;\ y=\underset{y'\in\{1,2,...,L\}}{arg\,max}\ \Lambda_{y'};\ if\ |h_{cp,y}|^2\ P_T<I_{pu} \\ p_j^{EH*}=\dfrac{I_{pu}}{|h_{cp,j}|^2}, p_x^{EH*}=0\ \forall x\neq j;\ j=\underset{j'\in\{1,2,...,L\}}{arg\,max}\ \Lambda_{j'}\dfrac{I_{pu}}{|h_{cp,j'}|^2}; if\ \dfrac{I_{pu}}{|h_{cp,j}|^2}<P_T \\ p_m^{EH*},\ p_n^{EH*},\ p_x^{EH*}=0\ \forall x\neq m,n;\ m,n=\underset{m',n'\in\{1,2,...,L\}}{arg\,max}\ U_{m',n'}; otherwise \end{cases} \quad (35)$$

Proposition 1: If $R_{cr}^1<R_{rs}^2$, it means that the throughput of the secondary network is limited by R_{cr}^1. Thus, $R=R_{cr}^1$ is the optimal throughput for (P1). Furthermore, optimal power allocations in (28) and (29) are determined as $\{p_l^*\}=\{p_l^{a*}\}$ and $p_r^*=p_r^{b*}$, respectively.

Proposition 2: If $R_{cr}^1>R_{rs}^2$, at first, the maximum throughput that can be provided for the relay-SU link is computed. To this issue, the total power that can be harvested by the relay is maximized as

$$\text{(P4)}\ \max_{\{p_l^{EH}\}}\ \zeta\rho\left(\sum_{l=1}^{L}\Lambda_l\,p_l^{EH}\right)\ \text{s.t. (9), (10), (15).} \quad (34)$$

Due to the convexity of (P4), using the optimal KKT conditions and a process similar to Lemmas 1 and 2, the optimal power allocations can be achieved as (35), where p_m^{EH*}, p_n^{EH*}, and $U_{m,n}$ denote as

$$p_m^{EH*}=\frac{I_{pu}-|h_{cp,n}|^2\,P_T}{|h_{cp,m}|^2-|h_{cp,n}|^2}, p_n^{EH*}=\frac{I_{pu}-|h_{cp,m}|^2\,P_T}{|h_{cp,n}|^2-|h_{cp,m}|^2}, \quad (36)$$

$$U_{m',n'}=\frac{\zeta\rho\left(\left(\Lambda_{m'}-\Lambda_{n'}\right)I_{pu}-\left(|h_{cp,n'}|^2\,\Lambda_{m'}-|h_{cp,m'}|^2\,\Lambda_{n'}\right)P_T\right)}{|h_{cp,m'}|^2-|h_{cp,n'}|^2}. \quad (37)$$

Based on (35), p_r^{EH*}, R_{cr}^3, and R_{rs}^4 can be written as

$$p_r^{EH*}=min\left(\zeta\rho\left((\sum_{l=1}^{L}\Lambda_l\ p_l^{EH*})+P_p\,\|\mathbf{g}_{pr}\|^2\right),\frac{I_{pu}}{\|\mathbf{h}_{rp}\|^2}\right). \quad (38)$$

$$R_{cr}^3=\sum_{l=1}^{L}\log_2\left(1+\frac{(1-\rho)\Lambda_l\ p_l^{EH*}}{\sigma^2+(1-\rho)P_p\left\|\mathbf{g}_{pr}\right\|^2}\right). \quad (39)$$

$$R_{rs}^4=\log_2\left(1+\frac{(1-\theta)\ p_r^{EH*}\|\mathbf{g}_{rs}\|^2}{\sigma_s^2+(1-\theta)P_p\ |g_{ps}|^2}\right). \quad (40)$$

Here, R_{rs}^4 is the maximum throughput that can be available on the relay to the SU link. Thus, if $R_{cr}^1>R_{rs}^2$ and $R_{rs}^4<R_{cr}^3$, it can be easily concluded that the throughput of the secondary network is limited by R_{rs}^4 and the condition (33) cannot be met equally as $R_{cr}=R_{rs}$. In this proposition, $R=R_{rs}^4$ is the optimal throughput for (P1). Also, optimal power allocations in (28) and (29) are determined as $\{p_l^*\}=\{p_l^{EH*}\}$ and $p_r^*=p_r^{EH*}$, respectively.

Table II. Algorithm 1

OPA for problem (P1)
1: Initialize $\psi'_{1_{min}}$, $\psi'_{1_{max}}$, $\xi'_{1_{min}}$, $\xi'_{1_{max}}$, ε_0, ε_1, ε_2, ε_3.
2: Obtain $\{p_l^{a*}\}$ and R_{cr}^1 from (21)-(24) in section 3.1.
3: Compute p_r^{b*} and R_{rs}^2 respectively from (26) and (27) in section 3.2.
4: **Based on Proposition 1**:
5: Set $\{p_l^*\}=\{p_l^{a*}\}$ and $p_r^*=p_r^{b*}$ as final power allocations, and $R=R_{cr}^1$ as an optimal throughput.
6: **Based on Proposition 2**:
7: If $R_{cr}^1>R_{rs}^2$ then
8: Compute $\{p_l^{EH*}\}$ from (35).
9: Based on (35), compute p_r^{EH*}, R_{cr}^3, and R_{rs}^4 respectively from (38)-(40).
10: Set $\{p_l^*\}=\{p_l^{EH*}\}$ and $p_r^*=p_r^{EH*}$ as final power allocations, and $R=R_{rs}^4$ as an optimal throughput.
11: **Based on Proposition 3**:
12: If $R_{rs}^4>R_{cr}^3$ then
13: Initialize $R_{cr}=R_{cr}^1$ and $R_{rs}=R_{rs}^2$.
14: While $\left\|R_{cr}-R_{rs}\right\|>\varepsilon_0$
15: Initialize $\Delta R=\varepsilon_1\left\|R_{cr}-R_{rs}\right\|$ and $R'_{cr}=R_{cr}$.
16: While $\left\|R_{cr}-R'_{cr}-\Delta R\right\|>\varepsilon_2\Delta R$
17: Initialize $\lambda'=\lambda'+\varepsilon_3$.
18: Compute $\{p_l^*\}$ from (41) similar to process of Lemmas 1 and 2.
19: Update R'_{cr} from (24) by substituting $\{p_l^*\}$.
20: End while

21: Update R_{cr} and p_r^* respectively from (24) and (26) by substituting $\{p_l^*\}$.
22: Update R_{rs} from (27) by substituting new p_r^*.
23: End while
24: Set $R = R_{cr} = R_{rs}$.
25: End if
26: End if

Proposition 3: If conditions $R_{cr}^1 > R_{rs}^2$ and $R_{rs}^4 > R_{cr}^3$, it can be concluded that condition $R_{cr} = R_{rs} = R$ is established by planning an appropriate power allocation. In the following procedure, R_{cr}^1 and R_{rs}^2 are set as the initial values of R_{cr} and R_{rs}, respectively. To obtain the optimum solution with the satisfaction of all constraints in (P1) as optimality conditions (28)-(33), R_{cr} can be cautiously reduced to increase R_{rs} until $R_{cr} = R_{rs}$. Based on (28), the power allocation is recast to the following form

$$p_l^* = \left(\frac{1}{ln2(\psi_1' + \xi_1' |h_{cp,l}|^2 - \lambda' \zeta \rho \Lambda_l)} - \frac{\sigma^2 + (1-\rho) P_p \left\| \mathbf{g}_{pr} \right\|^2}{(1-\rho)\Lambda_l} \right)^+, \quad (41)$$

where $\psi_1' = \frac{\psi_1}{\alpha}$, $\xi_1' = \frac{\xi_1}{\alpha}$, and $\lambda' = \frac{\lambda}{\alpha}$ are determined to satisfy the constraints (9), (10) and equality $R_{cr} = R_{rs}$, respectively. To ensure the convergence of our proposed algorithm, R_{cr} is reduced by a small step size ΔR, which is updated in each iteration according to the difference of R_{cr} and R_{rs}. To this end, λ' must raise by a small step size, and the optimum values of ψ_1' and ξ_1' can be found through the similar strategy in section 3.1. It should be noted that the increase in λ' continues until $R_{cr} - R_{cr}' - \Delta R$ is close to ΔR. Each of the values R_{cr}, R_{cr}', and ΔR are updated in the inner and outer loops of the algorithm. Next, the problem (P3) in section 3.2 must be solved again based on the derived $\{p_l^*\}$, and the obtained power assignment p_r^* also satisfies the condition (29). As a result, the current p_r^* increases R_{rs} in each outer loop. Therefore, this process of decreasing R_{cr} through increment of λ' continues until $R_{cr} = R_{rs}$ is almost satisfied. A detailed optimal proposed algorithm (OPA) is summarized in Table II.

4. Simulation and numerical results

In this section, the performance of the OPA is appraised via MATLAB numerical simulations. The computer system specifications are as follows: Intel Core(TM) i7-8550U CPU @ 1.80–1.99 GHz, Windows 10 with RAM 12 GB. The network model is considered as depicted in Fig. 1 and the simulation values set as Table III.

For comparison, the problem (P1) is solved by MATLAB CVX solver as the first benchmark. Furthermore, a low-complex EPA-IL (equal power allocation with respect to interference limit) algorithm is considered as the second benchmark. In the EPA-IL algorithm, the maximum power that can be assigned to any spatial subchannel is obtained by decomposing combinatorial constraints in (P2) to the individual constraints.

$$p_l^{equal*} = min\left(\frac{P_T}{L}, \frac{I_{pu}}{L.|h_{cp,1}|^2}, ..., \frac{I_{pu}}{L.|h_{cp,L}|^2} \right), \quad (42)$$

From (26), the power p_r^{equal*} can be assigned to the relay-SU link as

$$p_r^{equal*} = min\left(\zeta\rho\left((\sum_{l=1}^{L} \Lambda_l \; p_l^{equal*}) + P_p \| \mathbf{g}_{pr} \|^2 \right), \frac{I_{pu}}{\| \mathbf{h}_{rp} \|^2} \right). \quad (43)$$

Table III. Simulation values

Parameter	Value
P_T, P_p	30 dBm
N_T, N_R	4
ρ, θ	0.5
ζ	1
T	1 s
The Boltzmann constant (KT)	4.14×10^{-21} J
The carrier frequency (f_c)	2.4 GHz
The signal bandwidth (B)	1 MHz
Path loss exponent (s)	2
Noise figure (N_0)	5
The SU's antenna	1
σ_{rf}^2	$(1-\rho)KTB$
$\sigma_{rf,s}^2$	$(1-\theta)KTB$
$\sigma_{id}^2, \sigma_{id,s}^2$	$N_0 KTB$
The distance CBS-relay link (d_{cr})	3 m
The distance relay-SU link (d_{rs})	2 m
Fading type	Small scale
The distance CBS-PU and relay-PU	10 m
The distance PBS-all users	So far away (6 Km)
Channel coefficients	Rayleigh distribution
Number of Monte Carlo simulation	1000

Figure 2 illustrates the averaged sum throughput of the secondary network versus different interference limits I_{pu}. As expected, the averaged sum throughput of all algorithms becomes larger as the interference limit grows until saturated at a high regime. This is because that the power assignment at CBS and relay is limited by

interference power and power budget constraints respectively at low and high levels of I_{pu}. It can also be seen that the OPA outperforms the EPA-IL algorithm and converges to the CVX solver algorithm. A noteworthy observation is that the OPA performs slightly better in low threshold levels than the CVX solver algorithm and shows a higher average sum throughput. Additionally, the OPA in Fig. 3 has much less convergence time. The interference power constraints are inactive at high limits of I_{pu} and the

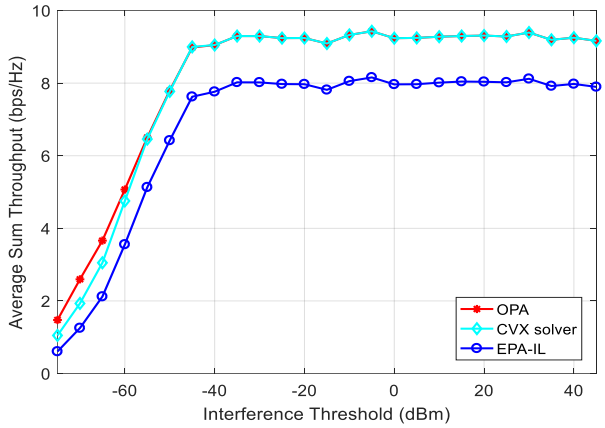

Fig. 2. The averaged sum throughput of the secondary network versus different interference limits I_{pu}

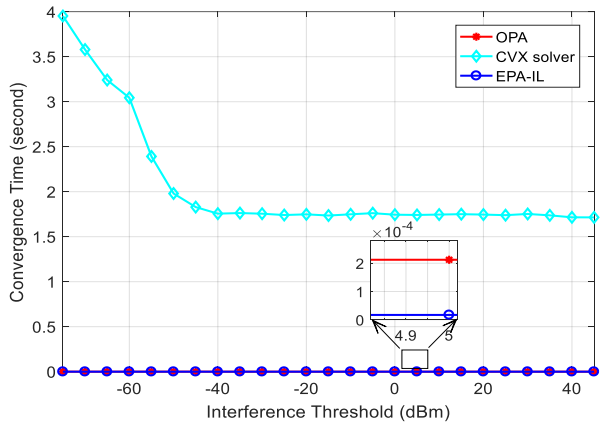

Fig. 3. The averaged convergence time behavior of the OPA, CVX solver, and EPA-IL algorithms versus different interference limits I_{pu}

sum throughput is limited by the power budget. So, the sum throughput values will be almost constant within these levels.

Figure 3 evaluates the averaged convergence time behavior of the OPA, CVX solver, and EPA-IL algorithms versus different interference limits I_{pu}. By comparing Fig. 2 and Fig. 3, the OPA not only provides almost the same sum throughput as the CVX solver algorithm, but also approaches the optimum point about 10000 times faster. Also, the convergence time of the simple EPA-IL algorithm is close to the OPA, but it offers much less sum throughput.

We measure the percentage of compliance with constraints through the proposed and CVX solver algorithms in Fig. 4. One remarkable observation is that the OPA simultaneously satisfies the constraints 100% at all thresholds, while the CVX solver algorithm only meets 40% to 90% of the constraints at the lower to middle thresholds. In the high interference limits, the interference power constraint will be inactive, and the CVX solver easily converges to the feasible optimum solution at 100% of tests. Although, this truth can be seen in Fig. 3 that the averaged convergence time of the CVX solver has converged to a constant value. In some scenarios, improper compliance with the constraints in

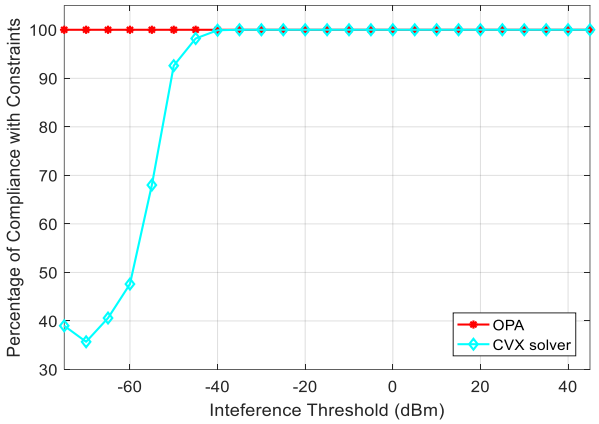

Fig. 4. Percentage of compliance with constraints through the proposed and CVX solver algorithms

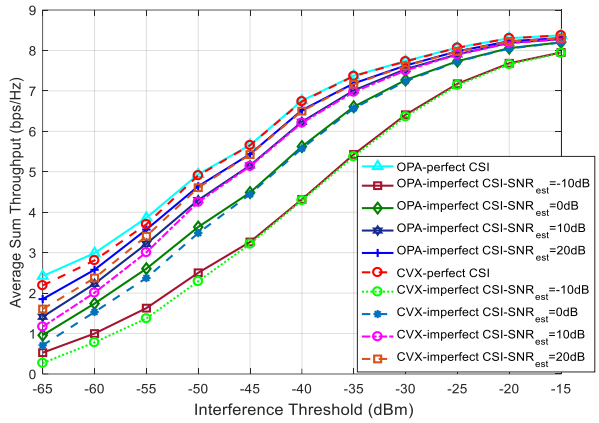

Fig. 5. The averaged sum throughput of the secondary network with imperfect CSI of the CBS-PU link versus different interference limits I_{pu}

the CVX solver may cause problems for the primary and secondary networks.

Figure 5 displays the effect of the imperfect CSI of the CBS-PU link on secondary network's averaged sum throughput versus different interference limits I_{pu}. Here, simulations are implemented for different SNR_{est}. SNR_{est} denotes the power ratio of the imperfect CSI of the CBS-PU channel to the perfect CSI of the CBS-PU channel. Despite imperfect CSI of the primary network, the OPA still outperforms CVX solver solution at low limits I_{pu} and converges to the CVX solver solution at high limits of I_{pu}. The reason for this superiority at low limits of I_{pu} is that due to the small threshold of interference in these areas, it is beyond the accuracy of the CVX solver. Therefore, the OPA can calculate the

power values more precisely at these low thresholds, where the interference constraint is active. Due to its higher accuracy, and as a result, it achieves a higher averaged sum throughput in these areas. As we expected, due to the interference constraint, the imperfect CSI of the CBS-PU channel reduces the sum throughput at low thresholds. The interference constraint is inactive at high limits of I_{pu}, so the imperfect CSI of the CBS-PU channel will not have much effect on the sum throughput.

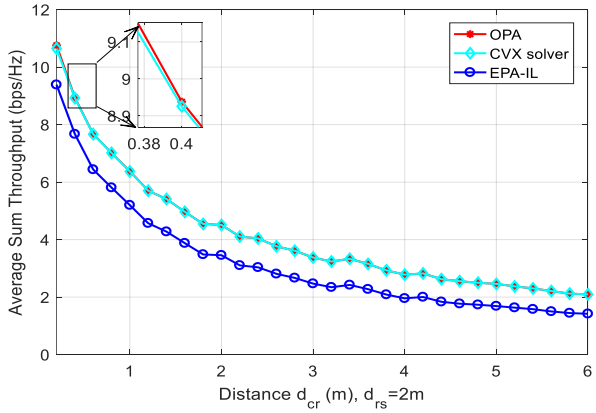

Fig. 6. The averaged sum throughput of the secondary network versus different distances between CBS-relay as d_{cr} with $d_{rs} = 2$ m and $I_{pu} = 0.001$

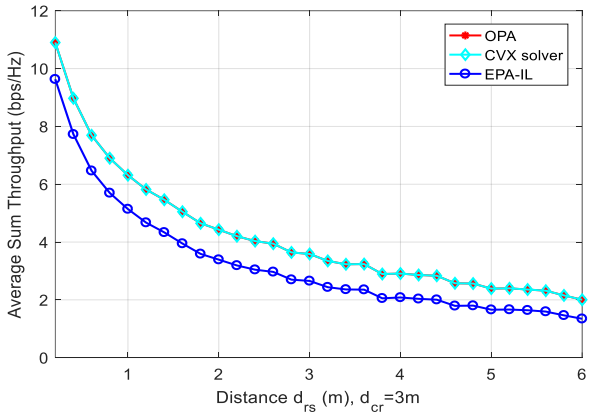

Fig. 7. The averaged sum throughput of the secondary network versus different distances between relay-SU as d_{rs} with $d_{cr} = 3$ m and $I_{pu} = 0.001$

The effect of CBS-relay and relay-SU distances is investigated in Fig. 6 and Fig. 7, respectively. As we can see, if relay closes to CBS with a fix distance d_{rs}, its harvested energy will be more that results in higher averaged sum throughput. For a fix distance d_{cr}, the averaged sum throughput will also be higher in the case of SU closes to relay. The OPA has a slightly better performance in; sum throughput than the CVX solver algorithm and is further away from the EPA-IL algorithm.

5. Conclusion

In this paper, we proposed an efficient power allocation algorithm for downlink MIMO DF relay-based SWIPT cognitive radio networks. The proposed algorithm is designed to maximize the secondary network sum throughput and meet the practical constraints. The problem is formulated as an optimization problem, and then the Lagrangian duality method is applied to solve it optimally. First, the main problem is divided into two optimization problems in two hops of the relay. Second, we use two lemmas to find the optimal power allocation in the first hop of the relay. Then, three propositions are considered based on these subproblems to find the main problem optimum solution. Based on this strategy, the innovative algorithm is proposed to attend a near closed-form answer. The simulation results confirm that our proposed algorithm not only operates so fast, but also competes with benchmarks in terms of achieving higher sum throughput. Contrary to expectation, it works even better than the CVX solver algorithm in some cases. The OPA is about 10000 times faster than the CVX solver. Additionally, the sum throughput especially at low thresholds increases by ~15-25% compared to the benchmark algorithms. Moreover, the constraints and objective function in OPA are 100% satisfied. As a vision for the future, the proposed algorithm can be developed to cover more relays, secondary users, or AF relays.

6. References

[1] Y. Xu, G. Gui, H. Gacanin, F. Adachi, “A survey on resource allocation for 5G heterogeneous networks: Current research, future trends, and challenges”, *IEEE Communications Surveys & Tutorials*, vol. 23, no. 2, pp. 668-695, 2021.

[2] Y.C. Liang, Y. Zeng, E.C. Peh, A.T. Hoang, “Sensing-throughput tradeoff for cognitive radio networks”, *IEEE transactions on Wireless Communications*, vol. 74, no. 4, pp. 1326-1337, 2008.

[3] M. Hasegawa, H. Hirai, K. Nagano, H. Harada, K. Aihara, “Optimization for centralized and decentralized cognitive radio networks”, *Proceedings of the IEEE*, vol. 102, no. 4, pp. 574-584, 2014.

[4] Z. Na, Y. Wang, X. Li, J. Xia, X. Liu, M. Xiong, W. Lu, “Subcarrier allocation based simultaneous wireless information and power transfer algorithm in 5G cooperative OFDM communication systems”, *Physical Communication*, vol. 29, pp. 164-170, 2018.

[5] X. Lu, P. Wang, D. Niyato, E. Hossain, “Dynamic spectrum access in cognitive radio networks with RF energy harvesting”, *IEEE Wireless Communications*, vol. 21, no. 3, pp. 102-110, 2014.

[6] S. Park, H. Kim, D. Hong, “Optimization for centralized and decentralized cognitive radio networks”, *Proceedings of the IEEE*, vol. 12, no. 3, pp. 1386-1397, 2013.

[7] R. Zhang, C.K. Ho, “MIMO broadcasting for simultaneous wireless information and power transfer”, *IEEE Transactions on Wireless Communications*, vol. 12, no. 5, pp. 1989-2001, 2013.

[8] F. Benkhelifa, A.S. Salem, M.S. Alouini, “Rate maximization in MIMO decode-and-forward communications with an EH relay and possibly imperfect CSI”, *IEEE Transactions on Communications*, vol. 64, no. 11, pp. 4534-4549, 2016.

[9] J. Yan, Y. Liu, “A dynamic SWIPT approach for cooperative cognitive radio networks”, *IEEE*

Transactions on Vehicular Technology, vol. 66, no. 12, pp. 11122-11136, 2017.
[10] S. Chatterjee, S.P. Maity, T. Acharya, "Energy-spectrum efficiency trade-off in energy harvesting cooperative cognitive radio networks", *IEEE Transactions on Cognitive Communications and Networking*, vol. 5, no. 2, pp. 295-303, 2019.
[11] D. Tse, P. Viswanath, "Fundamentals of wireless communication", Cambridge university press, 2005.
[12] D. Mishra, G.C. Alexandropoulos, "Jointly optimal spatial channel assignment and power allocation for MIMO SWIPT systems", *IEEE Wireless Communications Letters*, vol. 7, no. 2, pp. 214-217, 2017.
[13] M. Soleimanpour-Moghadam, S. Talebi, "Relay selection and power allocation for energy-efficient cooperative cognitive radio networks", *Physical Communication*, vol. 28, pp. 1-10, 2018.
[14] G. Huang, W. Tu, "A high-throughput wireless-powered relay network with joint time and power allocations", *Computer Networks*, vol. 160, pp. 65-76, 2019.
[15] J. Wang, G. Wang, B. Li, Z. Lin, H. Wang, G. Chen, "Optimal power splitting for MIMO SWIPT relaying systems with direct link in IoT networks", *Physical Communication*, vol. 43, pp. 101169, 2020.
[16] S. Gautam, E. Lagunas, S. Chatzinotas, B. Ottersten, "Relay selection and resource allocation for SWIPT in multi-user OFDMA systems", *IEEE Transactions on Wireless Communications*, vol. 18, no. 5, pp. 2493-2508, 2019.
[17] R. Malik, M. Vu, "Optimal transmission using a self-sustained relay in a full-duplex MIMO system", *IEEE Journal on Selected Areas in Communications*, vol. 37, no. 2, pp. 374-390, 2018.
[18] B. Li, H. Cao, Y. Rong, T. Su, G. Yang, Z. He, "Transceiver optimization for DF MIMO relay systems with a wireless powered relay node", *IEEE Access*, vol. 7, pp. 56904-56919, 2019.
[19] F. Benkhelifa, A.S. Salem, M.S. Alouini, "Sum-rate enhancement in multiuser MIMO decode-and-forward relay broadcasting channel with energy harvesting relays", *IEEE Journal on Selected Areas in Communications*, vol. 37, no. 12, pp. 3675-3684, 2016.
[20] S. Golipour, R. Ghazalian, S.M.H Andargoli, "Throughput maximization method for SWIPT DF multi-relaying network with low computational complexity", *Physical Communication*, vol. 47, pp. 101378, 2021.
[21] S. Shirvani Moghaddam, "Outage analysis of energy harvested relay-aided device-to-device communications in Nakagami channel", *Journal of Communications Software and Systems*, vol. 14, no. 4, pp. 302-311, 2018.
[22] A.H. Abd El-Malek, M.A. Aboulhassan, M.A. Abdou, "Power allocation scheme and performance analysis for multiuser underlay full-duplex cognitive radio networks with energy harvesting", *IEEE Access*, vol. 6, pp. 59031-59042, 2018.
[23] S. Lee, R. Zhang, "Cognitive wireless powered network: Spectrum sharing models and throughput maximization", *IEEE Transactions on Cognitive Communications and Networking*, vol. 1, no. 3, pp. 335-346, 2015.
[24] J. Kim, H. Lee, C. Song, T. Oh, I. Lee, "Sum throughput maximization for multi-user MIMO cognitive wireless powered communication networks", *IEEE Transactions on Wireless Communications*, vol. 16, no. 2, pp. 913-923, 2016.
[25] M. Askari, V.T. Vakili, "Robust Beamforming and Power Allocation in CR MISO Networks with SWIPT to Maximize the Minimum Achievable Rate", *Wireless Personal Communications*, vol. 106, no. 2, pp. 927-954, 2019.
[26] M. Mohammadi, S.M.H. Andargoli, "Sum throughput maximization for downlink MIMO-OFDMA based cognitive radio networks in spectrum overlay model", In 8th International Symposium on Telecommunications (IST), September 2016, Iran, Tehran, pp. 72-77.
[27] M. Mohammadi, S.M.H. Andargoli, "Power optimization and subcarrier allocation for downlink MIMO-OFDMA based cognitive radio networks", *Wireless Networks*, vol. 24, no. 6, pp. 2221-2235, 2018.
[28] M. Mohammadi, S.M.H. Andargoli, "Resource allocation algorithm for downlink MIMO-OFDMA based cognitive radio networks in spectrum underlay scenario", *IET Communications*, vol. 14, no. 11, pp. 1811-1820, 2020.
[29] M. Eidzadeh, R. Ghazizadeh, M. Hadi, "Joint resource allocation and position optimization in NOMA-based multi-UAV wireless communication networks", *Tabriz Journal of Electrical Engineering*, vol. 51, no. 3, pp. 327-336, 2022.
[30] K. Adli Mehr, J. Musevi Niya, N. Akar, "A multi-rate queue management for delay-constrained non-orthogonal multiple access (NOMA) based secure cognitive radio network", *Tabriz Journal of Electrical Engineering*, vol. 51, no. 2, pp. 149-159, 2021.
[31] T.M. Hoang, X.N. Tran, N. Thanh, L.T. Dung, "Performance analysis of MIMO SWIPT relay network with imperfect CSI", *Mobile Networks and Applications*, vol. 24, pp. 630-642, 2019.
[32] M. Alibeigi, S.S. Moghaddam, "Sum-rate optimization constrained by consumed power for multi-antenna non-regenerative relay network", *International Journal of Sensors Wireless Communications and Control*, vol. 10, no. 2, pp. 143-152, 2020.
[33] B. Wang, J. Zhang, A. Host-Madsen, "On the capacity of MIMO relay channels", *IEEE Transactions on Information theory*, vol. 51, no. 1, pp. 29-43, 2005.
[34] L. Lu, G.Y. Li, A.L. Swindlehurst, A. Ashikhmin, R. Zhang, "An overview of massive MIMO: Benefits and challenges", *IEEE journal of selected topics in signal processing*, vol. 8, no. 5, pp. 742-758, 2014.
[35] S. Simoens, O. Muñoz-Medina, J. Vidal, A. Del Coso, "On the Gaussian MIMO relay channel with full channel state information", *IEEE Transactions on Signal Processing*, vol. 57, no. 9, pp. 3588-3599, 2009.
[36] S. Boyd, S.P. Boyd, L. Vandenberghe, "Convex optimization", Cambridge university press, 2004.